SAND2011-1749C

Note to reviewers:

This paper is not yet formatted to ASME specifications. I find that such formatting takes a lot of time, and I usually have some things to fix after review.

After review and updates, the paper will be formatted to ASME requirements.

Thanks you for your patience and service.

Thanks again,

Nolan Finch

Proceedings of ASME 2011 5th International Conference on Energy Sustainability & 9th Fuel Cell Science, Engineering and Technology Conference
ESFuelCell2011
August 7-10, 2011, Washington, DC, USA

ESFuelCell2011-54455

DRAFT

Uncertainty Analysis and Characterization of the SOFAST Mirror Facet Characterization System

Nolan S. Finch[1], Charles E. Andraka[2]

[1] Sandia National Laboratories, PO 5800 Albuquerque NM USA 87185-1127, (505) 284-5190,: nsfinch@sandia.gov

[2] Sandia National Laboratories, PO 5800 Albuquerque NM USA 87185-1127

Abstract

SOFAST (Sandia Optical Fringe Analysis Slope Tool) is a mirror facet characterization system based on fringe reflection technology, which has been applied to dish and heliostat mirror facet development at Sandia National Laboratories and at development partner sites. The tool provides a detailed map of mirror facet surface normals, compared to design and to fitted surfaces. In addition, the fitting process provides insights into systematic slope characterization, such as focal lengths, tilts, and twist of the facet.

In this paper we present a preliminary analysis of the sensitivities of the output measurements to variations of the physical setup input parameters. From this sensitivity study, we perform a basic linear uncertainty analysis. The measured parameters include the fitted shape parameters (focal lengths and twist) and the residuals (typically called slope error). We utilize empirical propagation of these errors through the calculations to the output measurements, based on the measurement of an Advanced Dish Development System structural gore point focus facet. Thus, this study is limited to the characterization of sensitivities of the SOFAST embodiment intended for dish facet characterization.

With reasonably careful setup, SOFAST is demonstrated to provide focal length characterization within 1% of actual. The local slope deviation measurement is accurate within 0.2 mrad, while the global slope residual is accurate within 0.02 mrad.

Background

SOFAST (Sandia Optical Fringe Analysis Slope Tool) has been developed for fast, detailed characterization of point-focus mirror facets [1]. The tool uses fringe reflection (Deflectometry) techniques to map target points, as seen by a camera reflected in the facet. Others [2, 3, 4] have used Deflectometry techniques to characterize trough, linear Fresnel, tower, and dish facets and entire systems. The fringe reflection and Deflectometry approaches can characterize an entire reflector surface with anywhere from 8 to 32 total video images of the facet, while various fringe patterns are displayed on the target area. Typically hundreds of thousands of points to millions of points are characterized on the surface in parallel processing. This provides unprecedented fidelity in the characterization of the surface slope of the mirror facets.

Prior to these new techniques, the defacto standard for mirror characterization by the National Laboratories has been the Sandia and NREL-developed VSHOT system [5,6]. Typically, 1000 to 3000 points are measured on a 1 m² facet. This data is fitted to a parabola or other representative surface shape description, and the residual

difference between the local measurements and the fitted model is reported as a standard deviation of the error magnitude.

The characterization of trough and linear Fresnel facets has primarily focused on "focus deviation" [7], or the percentage of the facet reflected energy that will hit the receiver tube when properly mounted. Dish systems require further information, as light that gets through the aperture hole but is improperly distributed due to systematic slope errors, such as focal length errors, can cause unwanted excessive peak flux on the receiver. Therefore, the VSHOT tool, as well as SOFAST, fit the slope data to a Zernike Polynomial [8, 5, 1], which returns 2-dimensional polynomial parameters. From these parameters, one can deduce the focal length of the facet in two directions, the tilt of the facet coordinate system relative to the measurement system, and the cross term, which can represent the rotation of any astigmatism (optical book) or the twist of a facet that is not a full parabola of revolution [1].

The typical fitting parabolic equation is shown as equation 1. The measured data in SOFAST is the slope data, or the first partial derivatives of equation 1, shown as equations 2 and 3.

$$z=Ax^2+By^2+Cxy+Dx+Ey+F \qquad (1)$$

$$\frac{\partial z}{\partial x} = 2Ax + C + Ey \qquad (2)$$

$$\frac{\partial z}{\partial y} = 2By + D + Ex \qquad (3)$$

In these equations, the focal lengths are 1/(4A) and 1/(4B). The C and D terms, for small facet tilts, can be interpreted as the tilt of the facet. The E term, for a full parabola of revolution, can be interpreted as the rotation of the astigmatism relative to the measurement axes [8]. However, we have proposed [1] that for a partial parabola, this term can also be interpreted as the end-to-end twist of the facet. "Slope Error" is more correctly termed the "residual", which is anything "left over" after comparing the measurements to the model. The model may be the design facet shape, or, in this case, the fitted facet shape. Regardless of interpretation of the terms, it is important that "slope error" residuals not be divorced from the model to which they are a residual. Thus, if the residual is relative to the fitted parabola, all of the terms of the parabola should be reported with the residual. It is also important that, if the residual is to be used as a normally-distributed error in a ray trace or other model, it is truly normal or near normal, and not contain systematic errors.

While the SOFAST and other Deflectometry tools provide extensive data, it is important to determine the sensitivities to input parameters and measurements, and the uncertainty of the reported results. An uncertainty analysis of the VSHOT system [6] indicated the uncertainty in the fitted focal lengths and the local and global (RMS) residual (slope error). The uncertainty was measured relative to a high quality telescope mirror. The focal length uncertainty was determined at +/-0.5%, and the RMS residual slope error at +/-0.1mrad. März [9] performed an empirical uncertainty analysis of the CSP Services Deflectometry system for the measurement of trough facets. The stated uncertainty was 0.5 mrad local uncertainty in the slope measurement, and <0.2 mrad RMS, determined by imaging a flat surface of water. März does not report an uncertainty in focal length fit, since the CSP Services system does not report a fitted focal length. The CSP Services system uses a projection screen target to capture data from a long-focal-length facet, such as heliostat and trough facets.

The current SOFAST system is geared toward dish point focus facets. As such, the target is a large LCD monitor, with the camera attached to the system. This removes the uncertainties associated with projector lens distortions and skew (keystone) distortions that may be caused in the setup of the projector. In addition, SOFAST relies on an analysis of the data and a few linear measurements to determine the orientation of the measurement system in the facet coordinate system, rather than a carefully surveyed physical setup. The SOFAST system uses a lens distortion model [10] and several linear physical measurements, all of which may

introduce error. In this paper, we will describe the input parameters that may have error, determine the sensitivities of the outputs to these input parameter errors, and propose a system uncertainty for the measured parameters

Methodology

In this paper, we make uncertainty estimations for SOFAST based on measurement sensitivity to input parameter variations. SOFAST inputs include camera calibration parameters, camera/target relative positioning, target size, and distance from the facet to the target. We also investigated the impact of uncertainty in the target return ray point on the output parameters. Nominal characterization data was taken for an ADDS facet [11] placed roughly two focal lengths away from the target and at two other locations: 2f + 2 meters and 2f + 4 meters. We surmised that the locations off 2f lead to larger target "images", and therefore can have different sensitivities than the measurements at the 2f region. The design focal length of the ADDS facet is 210 inches (5.33 m) and it has been shown to have less than one milliradian residual slope error [1]. Figure 1 below illustrates the test setup. Table 1 below provides nominal values for the input parameters included in the study.

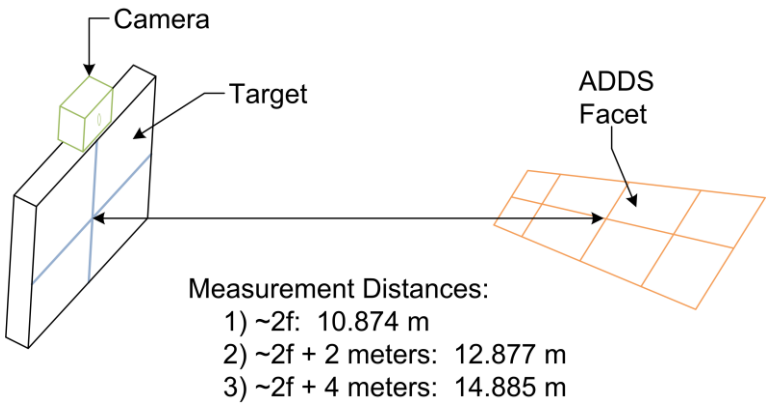

Figure 1. Testing Setup Illustration

Table 1. Input Parameters and Nominal Values

Input Parameter	Nominal Value	
Lens Barrel Distortion Parameter 1	-0.1526	-
Lens Barrel Distortion Parameter 2	1.9414	-
Lens Tangential Distortion Parameter 1	-0.0002	-
Lens Tangential Distortion Parameter 2	0.0009	-
Camera Focal Length, x	24.02	mm
Camera Focal Length, y	24.00	mm
Target/Camera Rotation, x	0	radians
Target/Camera Rotation, y	0	radians
Target/Camera Rotation, z	0	radians
Target/Camera Offset, x	-0.7739	meters
Target/Camera Offset, y	0.4304	meters
Target/Camera Offset, z	0.0508	meters
Target Dimension Horizontal	1.5478	meters
Target Dimension Vertical	0.8608	meters
Distance from Target to Facet	10.874, 12.877, 14.885	meters
Pixel Mapping Error	0	pixels

Fringe image data taken at these locations were reprocessed in SOFAST as each input was individually varied from its nominal value minus 10% to its nominal value plus 10% in fifty evenly-spaced increments. While a +/- 10% range is far larger than expected input uncertainties, evaluation over this large range allows an expanded view of the character of the impact of the uncertainty. Camera focal lengths were varied together to imitate image scaling errors. Target/camera relative rotations were varied from -0.5 radians to +0.5 radians as they are nominally zero. Characterization results from these SOFAST runs were used to calculate sensitivities by numerically taking a partial derivative of each output with respect to each varying input.

Sensitivities, combined with estimated input parameter uncertainties, were subsequently utilized to estimate the composite uncertainty of each measurement output. For example, measurement sensitivity to target width was calculated by varying target width from -10% of nominal to +10% of nominal which is a wide range. In practice, these measurements are good to within 3 mm so a uniform distribution (conservative assumption) for target width was set at nominal minus 3 mm to nominal plus 3 mm. Similar distributions were set for the remainder of inputs. Composite uncertainty was estimated by assuming each characterization output, y_i, is some non-linear function of the uniformly distributed input parameters, x_i.

$$y_i = f(x_1,....,x_n) \qquad (4)$$

The Taylor's Series expansion of (4) is (5) after dropping the higher order terms.

.

$$y_i \cong \left[\left.\frac{\partial f}{\partial x_1}\right|_{x_{10}} (x_1 - x_{10})\right] + ... + \left[\left.\frac{\partial f}{\partial x_n}\right|_{x_{n0}} (x_1 - x_{n0})\right] \qquad (5)$$

The partial derivatives in (5) are simply the sensitivities calculated above. The input parameters are assumed to be linearly independent and uniformly distributed across the conservative bounds estimated for each input. By the central limit theorem, y_i, the measurement output of interest, is approximately normally distributed with a standard deviation described by (6) and (7).

$$\mathrm{Var}(y) \cong \left(\left.\frac{\partial f}{\partial x_1}\right|_{x_{10}}\right)^2 \mathrm{Var}(x_1) + ... + \left(\left.\frac{\partial f}{\partial x_n}\right|_{x_{n0}}\right)^2 \mathrm{Var}(x_n) \qquad (6)$$

$$\mathrm{SD}(y) \cong \sqrt{\mathrm{Var}(y)} = \sqrt{\left(\left.\frac{\partial f}{\partial x_1}\right|_{x_{10}}\right)^2 \mathrm{Var}(x_1) + ... + \left(\left.\frac{\partial f}{\partial x_n}\right|_{x_{n0}}\right)^2 \mathrm{Var}(x_n)} \qquad (7)$$

$$\text{Where :} \quad \mathrm{Var}(x_i) = \frac{(x_{i\_\max} - x_{i\_\min})^2}{12}$$

Sensitivity Results

Sensitivities were calculated for every output variable with respect to every input variable at each measurement location. Figure 2, below, displays typical results for the affects of the target input parameters on the x focal length of the ADDS facet at measurement position one (2f). Sensitivities for each variable are simply the slopes of each line within the excepted uncertainty band of each input parameter.

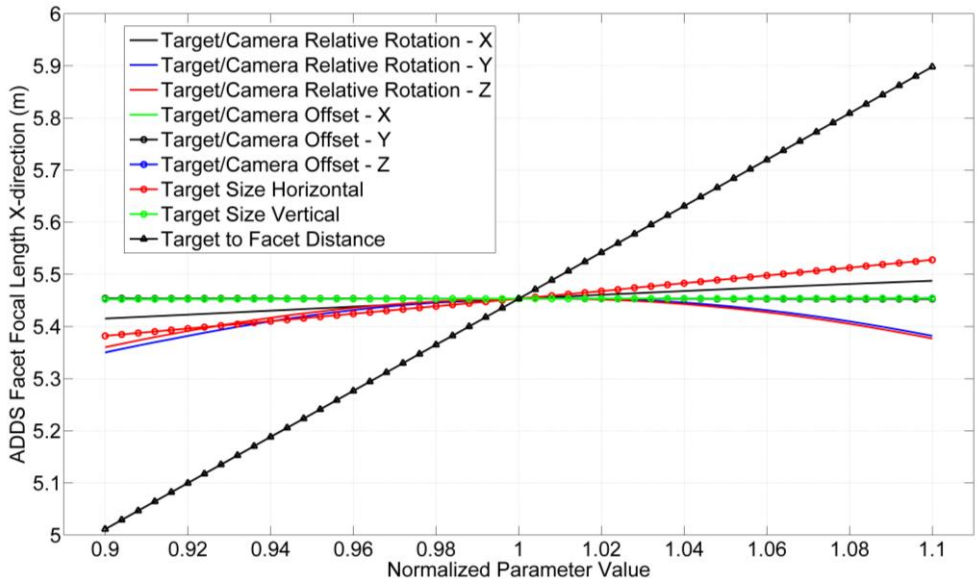

Figure 2. Sensitivity of ADDS Focal Length, X-Direction, to Target Input Parameter Variations

Figure 2 shows the relationship between variations in the target input parameters and the x-direction focal length of the ADDS facet as calculated by SOFAST. From this normalized plot, it is evident that SOFAST's characterization of the facet's x-direction focal length is relatively sensitive to the measurement of the distance between the facet and the target. It is also apparent that variations in target/camera relative rotations display a nonlinear relationship with facet focal length, x-direction. However, these non-linearities are exacerbated by the wide range of angles that were introduced for the sensitivity study. Within the range of uncertainties deemed reasonable for the target/camera relative rotations (discussed in the next section), linear approximations for sensitivity were readily made. Results for sensitivities of ADDS facet characterization outputs (focal lengths, twist metrics, and RMS slope error) with respect to inputs at measurement position one are shown below in Table 2.

Table 2. Input Parameter Sensitivity Results for Measurement Position One (2f)

Input Parameter	Sensitivity Values - Position One				
	Focal Length, X	*Focal Length, Y*	*Twist, X*	*Twist, Y*	*RMS Slope Error*
Lens Barrel Distortion Parameter 1	5.094E-02	1.857E-02	-8.536E-03	-4.226E-02	2.368E-01
Lens Barrel Distortion Parameter 2	7.176E-04	2.585E-04	-5.454E-04	-1.479E-03	3.866E-03
Lens Tangential Distortion Parameter 1	-9.326E-02	-4.997E-02	-1.705E+00	-9.240E+00	6.084E-02
Lens Tangential Distortion Parameter 2	1.305E-02	2.630E-02	-1.238E+00	-1.589E+00	6.160E+00
Camera Focal Length, x	1.498E-04	6.097E-05	4.834E-05	-3.967E-05	4.276E-04
Camera Focal Length, y	1.498E-04	6.097E-05	4.834E-05	-3.967E-05	4.276E-04
Target/Camera Rotation, x	7.359E-02	9.741E-02	-2.985E-01	-3.289E-02	-3.291E-02
Target/Camera Rotation, y	3.452E-02	5.138E-02	1.174E-01	-7.186E-01	1.617E-01
Target/Camera Rotation, z	1.745E-02	-4.505E-03	-5.045E+00	1.144E+01	2.493E-01
Target/Camera Offset, x	4.569E-03	2.897E-03	1.474E-01	1.197E-01	3.479E-02
Target/Camera Offset, y	-1.460E-02	-1.404E-04	9.244E-03	5.872E-02	5.231E-03
Target/Camera Offset, z	1.982E-01	2.252E-01	-1.219E-02	1.555E-02	-1.361E-01
Target Dimension Horizontal	4.717E-01	-8.248E-07	8.241E-02	1.334E-01	1.282E+00
Target Dimension Vertical	8.857E-03	2.677E-01	-1.384E-02	-4.510E-01	3.321E-01
Distance from Target to Facet	4.075E-01	4.620E-01	-2.109E-03	3.911E-02	-2.341E-01

As seen in Table 2, facet focal lengths are more sensitive to distance measurements and facet twist calculations are more sensitive to camera/target relative rotations. The overall impact of each input parameter on each facet measurement output is due to both the sensitivity of the input and the range of its uncertainty distribution which will be addressed in the next section. Due to this fact, many of the sensitivities shown in Table 1, such as the camera parameters, have a much smaller affect on measurement uncertainty than their sensitivities would indicate.

Sensitivities like those shown above were calculated for the two other facet measurements and the relative magnitude of sensitivities at each location compared. Figure 3, below, illustrates this sensitivity dependence by plotting the normalized magnitude of each output parameter versus measurement location. With the exception of RMS slope error, the characterization outputs become more sensitive to input variation as the facet is moved back from the 2f location (location one). Facet twist in the y-direction was almost unchanged from position one to position two.

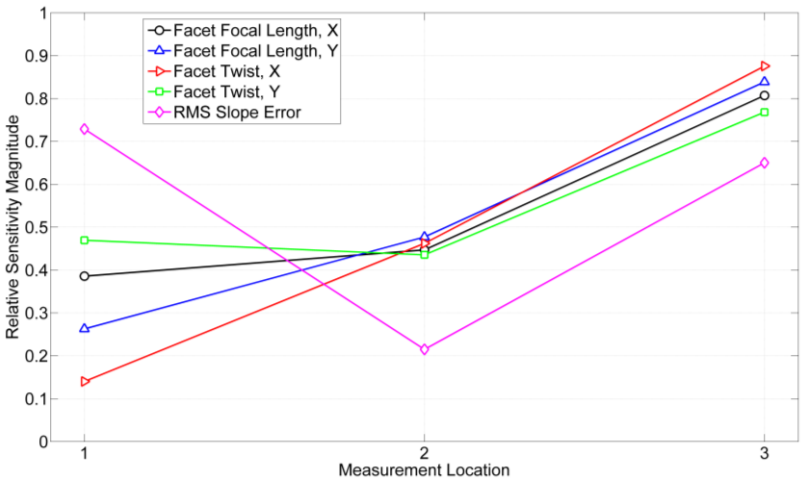

Figure 3. Relative Sensitivity Magnitude Versus Measurement Location

In addition to RMS slope error, it is also important to understand how local slope error changes with respect to varying input parameters as RMS slope error can mask directionality discrepancies that happen at the local level. To study local slope error deviations, eight representative points were selected from the ADDS facet – one from each subfacet – and slope errors in the x and y direction were tracked as input parameters varied. Figure 4 below illustrates the selected points. Figure 5 displays the variation in x-direction slope error at point

one as target input parameters are varied from nominal minus 10% to nominal plus 10% for data taken at 2f (measurement case one) .

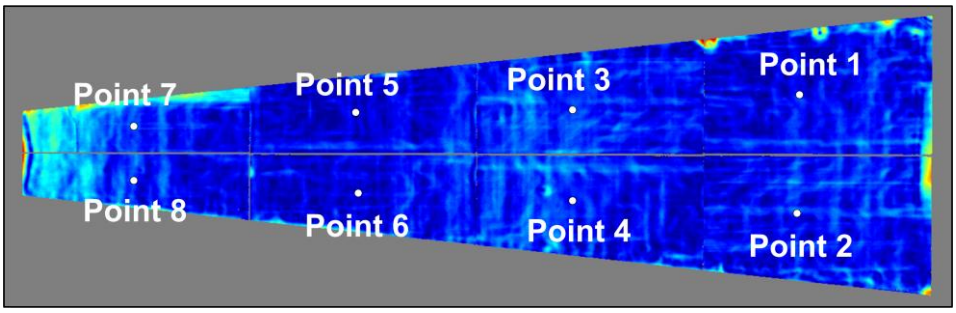

Figure 4. ADDS Facet RMS Slope Error with Points Used for Local Slope Error Sensitivity Analysis

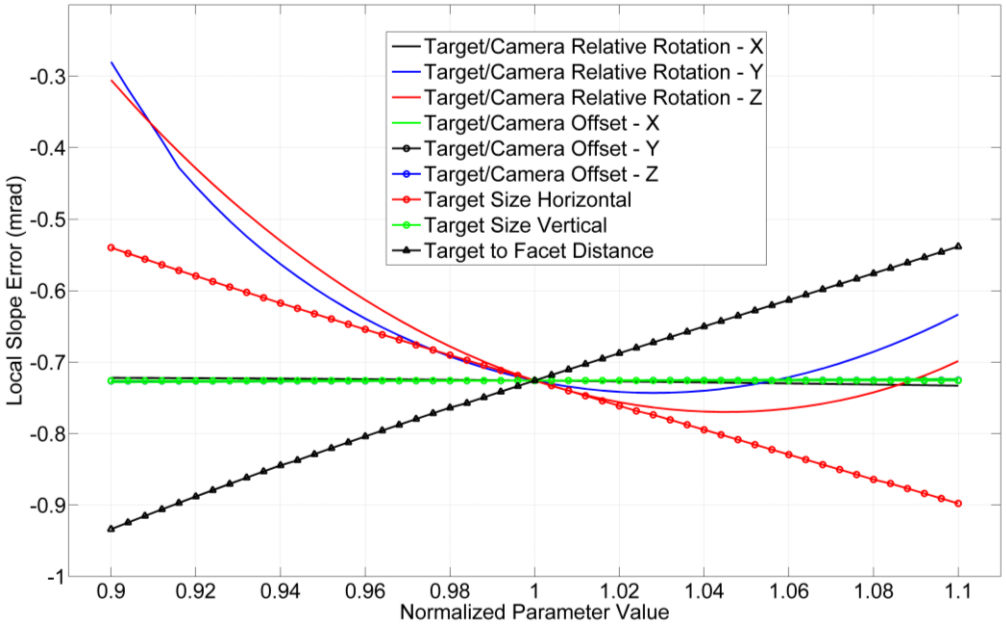

Figure 5. Local X-direction Slope Error at Point One (see Fig 4) for Data Taken at Measurment Location One (2f)

Using the same methodology mentioned above, sensitivities for both slope directions at all eight points were calculated and by finding a linear approximation of the sensitivity within the conservative uncertain distribution deemed reasonable for each input. Additional results for local slope error are included within the uncertainty analysis.

The analysis presented to this point has assumed that a pixel of interest on the camera array perfectly maps to a particular pixel on the display monitor (target) after being projected through the lens and reflected off the facet. As there will be uncertainty in this mapping, uncertainty was added to our "assumed-perfect" data and sensitivities were evaluated.

The local slope error (single point) was found to have a sensitivity of 0.037 mrad for each pixel spacing of error imposed, in both the horizontal and vertical directions. Discrete local errors imposed on just 8 of the pixel return locations had no impact on the determined facet focal length, twist, or global (RMS) slope error residual. When a normal distribution of error was applied to both axes of pixel return location, the sensitivity is about 0.01 mrad/pixel in both directions over a range of 0 to 10 pixels. However, the sensitivity appears to be parabolic,

and is only 0.002 mrad RMS/pixel over a range of 0 to 2 pixels of imposed error. The sensitivity to target pixel return location errors was only performed at the nominal 2f location. The errors would be correspondingly reduced by increasing the distance to the facet.

Uncertainty Results

By combining sensitivity information derived from simulation data and conservative estimates of input parameter distributions, it is possible to estimate facet characterization uncertainty. We have discussed the sensitivity results above – we now focus our attention on providing a rationale for our input variable distributions.

Camera calibration parameters (focal lengths and distortion coefficients) are calculated by imaging a checkerboard of known dimensions and processing these images with a piece of Sandia-developed software that is based on the CalTech calibration toolbox [10]. Estimates for camera calibration parameters provided by the toolbox also include uncertainty (standard deviation) estimates. We use these camera uncertainty estimates in our SOFAST uncertainty analysis.

Other inputs include physical setup parameters that describe the relative location of the camera, target, and facet. Linear measurements made by tape measure or laser-based distance finder are *conservatively* assumed to be uniformly distributed about nominal ± 3mm.

Target/camera relative rotations were actively driven to zero during setup by squaring the camera to the target. Pitch and yaw were zeroed using a laser square that projected a point onto a wall in front of the camera that represented the intersection of two planes orthogonal to the target. A preview of the camera with a crosshairs superimposed on the field of view was then used to align the camera to the laser projected point. The test setup was squared at a working distance of roughly 15 meters. Assuming our alignment was within two inches in pitch and yaw at this distance gives an uncertainty of 3 milliradians. Roll was set by leveling the target then finding a horizontally level fixture in the field of view of the camera. The camera was then manually rolled until the horizontal crosshair was aligned to the level object in the field of view. Assuming we were capable of sighting this line to within one inch accuracy at a distance of twelve feet leaves an uncertainty of 7 milliradians in roll.

Finally, we include pixel mapping errors described at the end of the sensitivity results section. We will assume a conservative uniform distribution for such errors centered about zero ± 10 pixels. Table 3 below summarizes the input distributions described here.

Table 3. Summary of Uncertainty Values and Distributions Used for Input Parameters

Input Parameter		Nominal	Uncertainty Parameter	Comment
Lens Barrel Distortion Parameter 1	-	-0.1526	σ = 0.0163	Standard Deviation Values Calculated During Camera Calibration
Lens Barrel Distortion Parameter 2	-	1.9414	σ = 0.7686	
Lens Tangential Distortion Parameter 1	-	-0.0002	σ = 0.0002	
Lens Tangential Distortion Parameter 2	-	0.0009	σ = 0.0003	
Camera Focal Length, x	mm	24.02	σ = 0.025	
Camera Focal Length, y	mm	24.00	σ = 0.025	
Target/Camera Rotation, x	radians	0	± 0.003 rad	Uniformly Distributed about Nominal
Target/Camera Rotation, y	radians	0	± 0.003 rad	
Target/Camera Rotation, z	radians	0	± 0.007 rad	
Target/Camera Offset, x	meters	-0.7739	± 3 mm	
Target/Camera Offset, y	meters	0.4304	± 3 mm	
Target/Camera Offset, z	meters	0.0508	± 3 mm	
Target Dimension Horizontal	meters	1.5478	± 3 mm	
Target Dimension Vertical	meters	0.8608	± 3 mm	
Distance from Target to Facet	meters	10.874, 12.877, 14.885	± 3 mm	
Pixel Mapping Error	pixels	0	± 10 pixels	

Using the information provided in Table 3 along with the sensitivity data previously presented allows uncertainty to be estimated for each of the output parameters at each of the measurement locations. Table 4 lists the approximate standard deviations for measure facet focal lengths, twist, and RMS slope error.

Table 4. Measurement Error Summary for Facet Focal Length, Twist, and RMS Slope Error

Measurement Location	Composite Uncertainty (Approximate Standard Deviations)						
	Focal Length, X (mm)	*Focal Length, Y (mm)*	*Twist, X (mrad/m)*	*Twist, Y (mrad/m)*	*RMS Slope Error (mrad)*	*Max Local Slope Error, X-direction (mrad)*	*Max Local Slope Error, Y-direction (mrad)*
Location One (2f)	1.52	1.08	2.04E-02	4.63E-02	5.81E-03	5.91E-02	5.95E-02
Location Two (2f+2m)	0.99	1.69	4.92E-02	1.41E-02	3.08E-03	5.85E-02	5.91E-02
Location Three (2f+4m)	1.59	2.91	1.00E-01	5.86E-02	2.57E-03	5.81E-02	5.91E-02

Table 4 shows that SOFAST focal length standard deviations are on the order of 1-3 mm for a facet with a design focal length of 5.33 meters. Twist uncertainty was much higher in relative terms and ranged from 0.01 mrad/meter to 0.1 mrad/meter depending on measurement location. Nominally measured twist for this facet was -0.09 and -0.3 mrad/meter in the x and y-directions respectively. RMS slope error standard deviation was on the order of microradians.

Local slope error uncertainty, even when taking pixel mapping errors into account, was also quite low. Uncertainties were calculated for the x and y-direction for eight points at all three locations. The maximum values for both the x and y-directions from the eight points are included in Table 4 and are all around 60 microradians.

Table 5 displays the final measurement summary for the ADDS facet included here. It displays the nominal measurement case for the ADDS facet then shows where ~99% of measurements would fall using worst case uncertainties from across the measurement locations. As previously mentioned, this assumes the input parameters included in this analysis are linearly independent and the output parameters are approximately normally distributed.

Table 5. Nominal Measurement Results and Worst Case Uncertainty Across the Measurment Locations

Parameter	Nominal	-3 Sigma	+3 Sigma
Flx (m)	5.453	5.427	5.479
Fly (m)	5.374	5.327	5.421
Twist X (mrad/m)	-0.092	-0.064	-0.119
Twist Y (mrad/m)	-0.296	-0.244	-0.348
RMS Slope Error (mrad)	0.812	0.798	0.827

References

[1] Andraka, C.E., Sadlon, S., Myer, B, Trapeznikov, K., Liebner, C., 2009, "Rapid Reflective Facet Characterization Using Fringe Reflection Techniques", *Proceedings of Energy Sustainability 2009*, San Francisco, CA, July 19-23.

[2] Heimsath, A., Platzer, W., Bothe, T., Wansong, L., 2008, "Characterization of Optical Components for Linear Fresnel Collectors by Fringe Reflection Method", *Proceedings of Solar Paces Conference*, Las Vegas, NV.

[3] Ulmer, S., Heller, P., Reinalter, W., 2008, "Slope Measurements of Parabolic Dish Concentrators Using Color-Coded Targets", *Journal of Solar Energy Engineering*, Vol 130, Transactions of the ASME #011015.

[4] Ulmer, S., Marz, T., Prahl, C, Reinalter, W., Belhomme, B., 2009, "Automated High Resolution Measurement of Heliostat Slope Errors", *Proceedings of Solar Paces Conference*, Berlin Germany, September 15-18.

[5] Jones, S.A, Neal, D.R., Gruetzner, J.K., Houser, R.M., Edgar, R.M., Kent, J., Wendelin, T.J., 1996, "VSHOT: A Tool for Characterizing Large, Imprecise Reflectors", *International Symposium on Optical Science Engineering and Instrumentation*, Denver, CO.

[6] Jones, S. A.; Gruetzner, J. K.; Houser, R. M.; Edgar, R. M.; Wendelin, T. J., 1997, "VSHOT Measurement Uncertainty and Experimental Sensitivity Study". *IECEC-97: Proceedings of the Thirty-Second Intersociety Energy Conversion Engineering Conference, 27 July - 1 August 1997, Honolulu, Hawaii. Volume 3: Energy Systems, Renewable Energy Resources, Environmental Impact and Policy Impacts on Energy*, American Institute of Chemical Engineers, New York, NY, **vol 3,** pp. 1877-1882.

[7] S. Ulmer, T. März, C. Prahl, W. Reinalter, B. Belhomme (2009)Automated High Resolution Measurement of Heliostat Slope Errors. *Proceedings of the SolarPACES conference*, 15-18 September 2009, Berlin, Germany.

[8] Malacara, Daniel, 1992, *Optical Shop Testing*, John Wiley & Sons, Inc., New York.

[9] Marz, T., Prahl, C., Ulmer, S., Wilbert, S., Weber, C., (2010)"Validation of two Optical Measurement Methods for the Qualification of the Shape Accuracy of Mirror Panels for Concentrating Solar Systems", *Proceedings of the SolarPACES conference*, September 21-24, Perpignan France.

[10] Bouguet, J-Y., 2008, "Camera Calibration Toolbox for Matlab", http://www.vision.caltech.edu/bouguetj/calib_doc/.

[11] Diver, R.B., and Andraka, C.E., 2003, "Integration of the Advanced Dish Development System", SAND2003-0780C, *International Solar Energy Conference Proceedings*, Kohala Coast, Hawaii Island, HI, March 15-18.